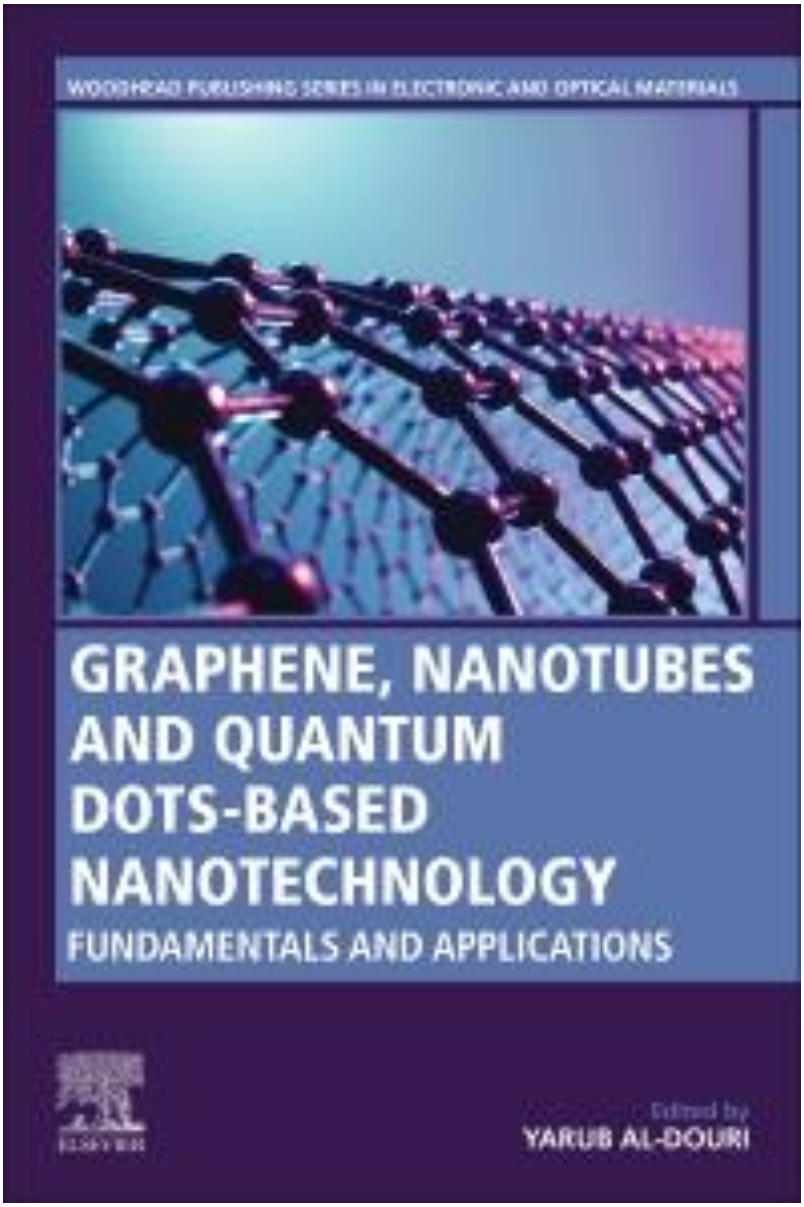

Graphene, Nanotubes and Quantum Dots-Based Nanotechnology

Fundamentals and Applications

Edited by:

Yarub Al-Douri

Woodhead Publishing Series in
Electronic and Optical Materials

Graphene, Nanotubes and Quantum Dots-Based Nanotechnology

Fundamentals and Applications

Edited by

Yarub Al-Douri
Engineering Department, American University of Iraq-Sulaimani, Sulaimani, Kurdistan, Iraq; Department of Mechatronics Engineering, Faculty of Engineering and Natural Sciences, Bahcesehir University, Besiktas, Istanbul, Turkey; Nanotechnology and Catalysis Research Centre, University of Malaya, Kuala Lumpur, Malaysia

WP
WOODHEAD
PUBLISHING
An imprint of Elsevier
elsevier.com/books-and-journals

Woodhead Publishing is an imprint of Elsevier
50 Hampshire Street, 5th Floor, Cambridge, MA 02139, United States
The Boulevard, Langford Lane, Kidlington, OX5 1GB, United Kingdom

Notices

Knowledge and best practice in this field are constantly changing. As new research and experience broaden our understanding, changes in research methods, professional practices, or medical treatment may become necessary.

Practitioners and researchers must always rely on their own experience and knowledge in evaluating and using any information, methods, compounds, or experiments described herein. In using such information or methods they should be mindful of their own safety and the safety of others, including parties for whom they have a professional responsibility.

To the fullest extent of the law, neither the Publisher nor the authors, contributors, or editors, assume any liability for any injury and/or damage to persons or property as a matter of products liability, negligence or otherwise, or from any use or operation of any methods, products, instructions, or ideas contained in the material herein.

ISBN: 978-0-323-85457-3

Publisher: Matthew Deans
Acquisitions Editor: Kayla Dos Santos
Editorial Project Manager: Fernanda A. Oliveira
Production Project Manager: Kamesh Ramajogi
Cover Designer: Miles Hitchen

Typeset by Aptara, New Delhi, India

Contents

Optical properties of quantum dots

26

Yarub Al-Douri[a,b,c] *and Rajan Jose*[d]
[a] Engineering Department, American University of Iraq-Sulaimani, Sulaimani, Kurdistan, Iraq, [b] Department of Mechatronics Engineering, Faculty of Engineering and Natural Sciences, Bahcesehir University, Besiktas, Istanbul, Turkey, [c] Nanotechnology and Catalysis Research Centre, University of Malaya, Kuala Lumpur, Malaysia, [d] Nanostructured Renewable Energy Materials Laboratory, Faculty of Industrial Sciences & Technology, Universiti Malaysia Pahang, Kuantan, Pahang, Malaysia

26.1 Introduction

The semiconductors are interesting materials in solid-state physics. The most widely studied materials are Groups IV and II–VI. These materials have different band gaps that are usually extending from few to several electron volts and whose temperature coefficient $dE_g = dT$ is positive, and they have high mobility [1]. They are showing interesting in optoelectronic applications [2]. It is advantageous to use the computational method based on total energy calculations to study the phase transition from the coordinated number Nc = 4- to 6-fold [3]. Third-generation approaches to photovoltaics (PVs) aim to decrease costs and significantly increasing efficiencies but maintaining the economic and environmental cost advantages of thin-film deposition techniques [4]. There are several approaches to achieve such multiple energy threshold devices [5]; tandem or multicolor cells, concentrator systems, intermediate-level cells, multiple carrier excitation, up/down conversion, and hot carrier cells [6].

Billaud and Truong [7] have computed the ground state Lamb shift of a semiconductor spherical quantum dot in the effective mass approximation. It appears to be significant enough to be detectable for a wide range of small quantum dots synthesized in semiconductors. They have suggested the Casimir effect to observe it. While Thu and Voskoboynikov [8] have calculated the lowest energy states of electrons confined in an asymmetrical InAs/GaAs double lens-shaped quantum dot molecule in external magnetic field. Based on the effective three-dimensional one electronic-band Hamiltonian approximation, the electronic energy states of the system were computed by nonlinear iterative method using Comsol MultiPhysics package. This description allows them to simulate the semiconductor quantum dot molecule in arbitrary directed magnetic field. Simulation results clearly have showed that the diamagnetic shifts of the electronic energy levels are anisotropic and nonuniform. Therefore, they have demonstrated an opportunity to dynamically manipulate electronic states not only by varying the magnitude but also by changing the direction of the magnetic field. Moreover, Lam and Ng [9] have used bio-tags to emit different color light with different dot sizes, and quantum dots are currently extensively studied for application

Graphene, Nanotubes and Quantum Dots-Based Nanotechnology: Fundamentals and Applications.
DOI: https://doi.org/10.1016/B978-0-323-85457-3.00029-3

as quantum devices taking advantage of the artificial atom" properties, such as their discrete energies, electron spins, and quantum transport energies. The self-assembled semiconductor quantum dots are grown on the wetting layer of a few monolayer thickness and subsequently capped with a strain-reduction layer covering the dots to stabilize them. They have studied the indium arsenide/gallium arsenide self-assembled quantum dots modeled with a wetting layer between the quantum dot and substrate, and the strain-reducing capping layer above the quantum dot. They have introduced a new model with an interfacial layer between the quantum dot and the capping layer and investigate the effective mechanical and electronic properties using the finite element method and deformation potential theory. However, Udipi et al. [10] have presented semiclassical simulation results for the potential energy profile and electron density distribution in 200 nm silicon quantum dot. For the solution of the continuity equation, the efficient difference approximations proposed by Scharfetter and Gummel [11] have extended to three dimensions. In essence, they have followed the two-dimensional approach due to Selberherr et al. [12] extend two to three dimensions.

The investigation of further materials research is interesting when one tries to gain some information about the diameter dependence of the compounds; especially it is proved with some of the other materials [13,14]. It seems more fundamental to relate the diameter dependence behavior to the bonds between nearest atoms. By controlling the evolution with diameter dependence of the compound, it could attempt to link the effect of quantum dot diameter to the quantum dot potential. In this context, we have used this procedure for testing the validity of our model [15] of QDs potential. The obtained energy band gaps are used to calculate the quantum dot potential and to predict materials for QDs.

The aim of this chapter review is to present a comprehensive study of our model [15] for calculating the diameter dependence on QDs potential for different dot diameters for semiconductors using the full potential linearized augmented plane wave (FP-LAPW), analytical and characterization researches of thermal evaporation and chemical bath deposition techniques to investigate the structural and optical properties utilizing specific models for the elements, compounds, and alloys materials.

26.2 Quantum dots

The confinement can be due to electrostatic potentials (generated by external electrodes, doping, strain, impurities), the presence of an interface between different semiconductor materials (e.g., in core-shell nanocrystal systems), the presence of the semiconductor surface (e.g., semiconductor nanocrystal), or a combination of these. A quantum dot has a discrete quantized energy spectrum. The corresponding wave functions are spatially localized within the quantum dot but extend over many periods of the crystal lattice [13]. A quantum dot contains a small finite number (of the order of 1–100) of conduction band electrons, valence band holes, or excitons, i.e., a finite number of elementary electric charges. Small quantum dots, such as colloidal semiconductor nanocrystals, can be as small as 2–10 nanometers, corresponding to 10–50 atoms in diameter and a total of 100–100,000 atoms within the quantum dot volume. Self-assembled quantum dots are typically between 10 and 50 nm in size.

Quantum dots defined by lithographically patterned gate electrodes, or by etching on two-dimensional electron gases in semiconductor heterostructures can have lateral dimensions exceeding 100 nm. At 10 nm in diameter, nearly 3 million quantum dots could be lined up end to end and fit within the width of a human thumb. Simplifying things greatly (as this guide aims to do, mostly), quantum dots are incredibly small particles. They range between 2 and 10 nanometers in diameter, which is equivalent to 50 atoms. Yes, atoms. You cannot measure these things using your old-school shatter-proof ruler. It is this small size that gives quantum dots the unique properties to improve our tech. The color light that a quantum dot emits is directly related to its size; smaller dots appear blue, larger ones more red. In LCD screens, they are applied as a way of eliminating the need for White LED backlights and color filters [14,15].

Higher peak brightness—one of the reasons TV manufacturers like quantum dots is that they allow them to produce TVs with much higher peak brightness. This opens up some interesting possibilities, such as enabling support for "high dynamic range" TVs that support standards such as Dolby Vision. In simple terms, Dolby Vision is a film standard that, when used, results in content that retains more color and contrast information than existing standards. The result is pictures that have greater differences in the brightest and darkest parts of the image and look more "dynamic" and real as a result. Imagine shots were looking into the sun actually feels like looking in to the sun for real and you get an idea. To do this you need brighter TVs and quantum dots deliver exactly that. Following the acceptance of 4K resolutions, HDR, in general, is the next big feature of TVs, and all of the top TV sets announced at CES 2016 this year have made bold claims about their "high dynamic range" capabilities. Quantum Dot technology, like OLED, goes hand in hand with this advance [10,15].

26.3 Computational method

The LAPW method is utilized for solving the equations of density functional theory (DFT). Modern implementations allow for a number of approximations to exchange and correlation (LDA, generalized gradient approximation (GGA), and LDA+U, among others) and make no approximations to the shape of the crystal potential, unlike methods employing the atomic sphere approximation which assume spherical symmetry around each atom. Like most modern electronic-structure methods, the LAPW method is a variational expansion approach which solves the equations of DFT by approximating solutions as a finite linear combination of basis-functions. What distinguishes the LAPW method from others is the choice of basis. The LAPW basis is constructed to be particularly accurate and efficient for the solution of the all-electron *ab initio* electronic-structure problem, where solutions are rapidly varying and atomic-like (like isolated-atom solutions) near the atoms but more smoothly varying and not atomic-like throughout the rest of the cell.

The calculations were carried out using the full potential linearized augmented plane wave (FP-LAPW) method as implemented in WIEN2K code [16]. The exchange-correlation potential was treated using the GGA [17] for the total energy calculations, the Engel–Vosko GGA (EVGGA) formalism [18] and modified Becke Johnson (mBJ) [19] for principal energy calculations. To overcome the shortcoming of both LDA and

GGA of underestimation of the energy gap [20], we have used EVGGA and mBJ. This shortcoming is ascribed to the fact that they do not reproduce the exchange-correlation energy and its charge derivative correctly. Hence, the modified form of GGA is the EVGGA that is improved in mBJ, which is capable to better reproduce the exchange potential at the expense of less agreement in the exchange energy that yields a better band splitting [21–25]. In the FP-LAPW method, the wave function, charge density, and potential were expanded by spherical harmonic functions inside nonoverlapping spheres surrounding the atomic sites (muffin-tin spheres) and by plane waves basis set in the remaining space of the unit cell (interstitial region). The maximal l value for the wave function expansion inside the atomic spheres was confined to $l_{max} = 8$. The muffin-tin radii were assumed to be 2.0 atomic units (a.u.) for Pb, S, and Te. The plane wave cut-off of $K_{max} = 8.0/RMT$ was chosen for the expansion of the wave functions in the interstitial region for the PbS and PbTe binary compounds, while the charge density is Fourier expanded up to $G_{max} = 14$ $(Ryd)^{1/2}$. The irreducible wedge of the Brillouin zone was described by a mesh of 10 special *k*-points for binary compounds. The self-consistent calculations are converged since the total energy of the system is stable within 10^{-5} Ry. The FPLAPW has been proved to be one of the accurate methods of calculating the electronic properties within the DFT [26–29].

26.4 Experimental techniques

According to the following experimental steps, lead iodide was prepared by a reaction of potassium iodide (KI) with lead nitrate $Pb(No_3)_2$ [30]:

a) Pb $(No_3)_2$ solution of 0.01 M by dissolving 3.31 mg in 1000 mL of distilled water.

b) KI solution preparation with 0.05 M by dissolving 8.31 mg in 1000 mL of distilled water. Adding 50 ml of KI solution to 50 ml of $Pb(No_3)_2$ solutions to prepare PbI_2 will appear yellow lead iodide at the bottom of the beaker insoluble by water. Also, potassium nitrate (KNo_3) is dissolved by water. Afterthat, the water is discarded beyond drying deposited material. Finally, it is removed from the beaker to keep in desiccators.

$$Pb(No_3)_2 + KI \rightarrow PbI_2 + KNo_3 \tag{26.1}$$

PbI_2 nanostructures were grown on glass substrates at room temperature by Electron Beam Evaporation (Auto 306 Vacuum Coater, USA). The main reason of utilizing this method is to permit the large area deposition in cost-effective manner [11]. To measure the thickness, the weight method was used. Sensitive electrical balance (Metler AE-160, USA) was utilized, with precision reaching 10^{-4} g. The structural properties were investigated via X-ray diffractometer (XRD) to determine the crystallinity of sample, the diffraction for determining spacing, preferred orientation and the particle size. XRD system (Philips PW 1710 X-ray diffractometer, USA) has been used for the following: Source radiation of CuKα with 1.54 Å wavelengths, incidence angle: 10–60 degree, and scanning speed: (5 degree/min). The optical properties have been investigated by ultra-violet spectroscopy (UV-vis) at room temperature via Perkin-Elmer Lambda (950 spectrophotometer, USA) in the 300–1100 nm wavelength range.

Table 26.1 The calculated principal energy band gaps for Si (in eV) at different diameters (in nm) compared to other theoretical results and experimental data [13].

Dot diameter	E_g (Γ–Γ)	E_g (Γ–X)	E_g (Γ–L)
54.3	2.742	1.436; 1.11[a],[b]	2.028
54	2.747	1.396	2.094
53.6	2.751	1.352	2.164
53.3	2.757	1.272	2.279
53	2.752	1.345	2.174
52.7	2.759	1.233	2.332

[a] [36] expt.;
[b] [37].

Also, $ZnCl_2$ and Na_2S were used as zinc source and sulfur source, respectively. $ZnCl_2$, Na_2S, and mercaptoethanol (ME) were obtained from Sigma-Aldrich. ZnS nanomaterials were synthesized with chemical bath deposition technique with ME, as capping agent (or surface-active agent surfactant). The first 50 mL aqueous solution of $ZnCl_2$ (0.01 M) was prepared at room temperature, where, 50 mL aqueous solutions of ME with different concentrations (0.001, 0.1, 0.7 M) were added dropwise to the first solution under continuous stirring. Then, 50 mL of Na_2S (0.01 M) solution was added to the mixture. A three-neck reaction flask was used under N_2 inert gas to prevent any oxidation effect. While reaction was going on, a magnetic stirrer was used for continuous stirring of solution in the reaction vessel. The final solution was centrifuged and washed several times with double distilled water, to wash out the NaCl impurities. The remaining centrifuged ZnS was dried under a table lamp. The obtained powder was analyzed via XRD (Philips PW 1710 X-ray diffractometer, USA), UV-visible (Jobin Yvon model HR 800 UV system, Kyoto, Japan), and transmission electron microscopy (TEM) (Model JEOL JEM-100cx, Japan) techniques [31].

26.5 Results and discussion

26.5.1 Si element

Normally, the covalent semiconductors are fourfold coordinated. The reason that the density is so low and the nearest neighbors are bound by overlapping hybridized orbitals, which are the well-known sp^3 hybrids with tetrahedral direction [32]. Hence, it is possible to tune the band gaps using dot diameter. The calculated values of the direct (Γ→Γ) and the indirect (Γ → X) and (Γ→L) band gaps within EVGGA of the investigated Si-element at different diameters are listed in Table 26.1 along with the experimental data [33] and other previous theoretical calculation [34]. Our calculated value of the (Γ → X) bandgap is slightly overestimated compared to the available data. This could be attributed to our use of the EVGGA approximation. Due to these small values, Si has been classified as a narrow band gaps semiconductor. Because of their use in infrared light generation and detection, the bandgap variations of dot diameters represent an important property to study. As mentioned at Table 26.1, the band gaps

Index

Page numbers followed by "*f*" and "*t*" indicate, figures and tables respectively.

H